

Anisotropic conductivity of $\text{Nd}_{1.85}\text{Ce}_{0.15}\text{CuO}_{4-\delta}$ films at submillimeter wavelengths

A. Pimenov¹, A. V. Pronin¹, A. Loidl¹, U. Michelucci², A. P. Kampf², S. I. Krasnosvobodtsev³, V. S. Nozdrin³, and D. Rainer⁴

¹*Experimentalphysik V, EKM, Universität Augsburg, 86135 Augsburg, Germany*

²*Theoretische Physik III, EKM, Universität Augsburg, 86135 Augsburg, Germany*

³*Lebedev Physics Institute, Russian Acad. Sci., 117942 Moscow, Russia*

⁴*Physikalisches Institut, Universität Bayreuth, 95440 Bayreuth, Germany*

The anisotropic conductivity of thin $\text{Nd}_{1.85}\text{Ce}_{0.15}\text{CuO}_{4-\delta}$ films was measured in the frequency range $8 \text{ cm}^{-1} < \nu < 40 \text{ cm}^{-1}$ and for temperatures $4 \text{ K} < T < 300 \text{ K}$. A tilted sample geometry allowed to extract both, in-plane and c-axis properties. The in-plane quasiparticle scattering rate remains unchanged as the sample becomes superconducting. The temperature dependence of the in-plane conductivity is reasonably well described using the Born limit for a d-wave superconductor. Below T_C the c-axis dielectric constant ε_{1c} changes sign at the screened c-axis plasma frequency. The temperature dependence of the c-axis conductivity closely follows the linear in T behavior within the plane.

The electron-doped superconductor $\text{Nd}_{2-x}\text{Ce}_x\text{CuO}_4$ (NCCO) [1,2] reveals a number of properties, which are rather different from other cuprate superconductors. It has long been believed that the superconductivity in this compound is characterized by a s-wave order parameter (for a review see [3]). However, recent experiments, including phase-sensitive tricrystal [4] and penetration depth measurements [5,6], strongly support d-wave type symmetry.

In-plane microwave properties of NCCO have been investigated using resonator techniques [5,7–9]. The infrared conductivity has been obtained via Kramers-Kronig analysis of reflectivity data [10,11] and by thin film transmission [12]. In contrast to a number of ab-plane experiments, there exists only little information concerning the c-axis properties of NCCO, which is explained by the typically small dimensions of the samples along the c-axis. Most experiments on c-axis dynamics [13,14] were carried out using polycrystalline NCCO samples.

Recently we have demonstrated the possibility of using a tilted-sample geometry to extract the anisotropic conductivity of layered cuprates in the submillimeter frequency range [15]. This method combines the possibilities of the quasi-optical transmission geometry with the high anisotropy of NCCO which may be estimated by the resistivity ratio $\rho_c/\rho_{ab} \sim 10^4$ [16]. In this paper we present the in-plane and c-axis conductivity of an oxygen reduced $\text{Nd}_{1.85}\text{Ce}_{0.15}\text{CuO}_{4-\delta}$ film ($T_C=16.9 \text{ K}$, sample #A) in the submillimeter frequency range ($8 \text{ cm}^{-1} < \nu < 40 \text{ cm}^{-1}$) and for temperatures $4 \text{ K} < T < 300 \text{ K}$. Data on an optimally doped film [15] (sample #B, $T_C = 20.1 \text{ K}$) are also discussed.

The films were prepared using a two-beam laser deposition on YSZ substrates [17]. X-ray analysis showed the c-axis orientation of the films relative to the crystallographic axes of the substrate. The YSZ substrate of the presented film (#A) was tilted from the (001) orientation by an angle $\alpha = 2.6^\circ \pm 0.5^\circ$. Therefore, the film was also tilted by the same angle from the ideal c-axis orientation.

The oxygen concentration in the deposition chamber was reduced compared to the optimum value which resulted in a lower T_C of the film (#A). The ac-susceptibility measurements revealed an onset temperature of 16.9 K and a slightly broader transition width ($\Delta T[10\% - 90\%] = 2.0 \text{ K}$) as compared to the optimally doped film (sample #B: $\Delta T = 0.9 \text{ K}$ [15]).

The transmission experiments in the frequency range $6 \text{ cm}^{-1} < \nu < 40 \text{ cm}^{-1}$ were carried out in a Mach-Zehnder interferometer arrangement [18] which allows both the measurements of transmittance and phase shift. The properties of the blank substrate were determined in a separate experiment. Utilizing the Fresnel optical formulas for the complex transmission coefficient of the substrate-film system, the absolute values of the complex conductivity $\sigma^* = \sigma_1 + i\sigma_2$ were determined directly from the observed spectra. Using the tilted sample geometry at different polarizations of the incident radiation it was possible to separate the conductivity at a given tilt angle into ab-plane and c-axis components. The geometry of the experiments is shown in the insets in Fig. 1.

The conductivity of a tilted sample may be calculated assuming a free-standing film of thickness d in a uniform electromagnetic field $Ee^{-i\omega t}$ parallel to the surface. If the film is thin compared to the penetration depth, $d \ll \lambda$, then the current and field distributions may be considered to be uniform. Taking into account the charges formed at the surface, the following equations can be derived for the geometry given in the right inset of Fig. 1:

$$\begin{cases} j_a = \sigma_a [E \cos \alpha - (s/\varepsilon_0) \sin \alpha] \\ j_c = \sigma_c [-E \sin \alpha - (s/\varepsilon_0) \cos \alpha] \end{cases} \quad . \quad (1)$$

Here j_a (j_c) is the current density, σ_a (σ_c) is the complex conductivity in the ab-plane (along the c-axis), s is the surface charge density, ε_0 is the permittivity of free space, $\omega = 2\pi\nu$ is the angular frequency, and α is the tilt angle. An additional equation, $i\omega s + j_a \sin \alpha + j_c \cos \alpha = 0$, follows from the charge conservation. The effective conductivity of the film can be defined through $\sigma_{eff}E =$

$j_{eff} = j_x \cos \alpha + j_y \sin \alpha$. Solving these equations one obtains:

$$\sigma_{eff} = \frac{-i\varepsilon_0\omega(\sigma_a \cos^2 \alpha + \sigma_c \sin^2 \alpha) + \sigma_a \sigma_c}{-i\varepsilon_0\omega + \sigma_a \sin^2 \alpha + \sigma_c \cos^2 \alpha} . \quad (2)$$

Both σ_{eff} and σ_a can be determined experimentally using the geometry shown in the right and left insets of Fig. 1, respectively. Therefore Eq. (2) can easily be solved for the c-axis conductivity. Within the approximation $\alpha \approx \sin \alpha \ll 1$ and $|\sigma_a| \gg |\sigma_c|$, Eq. (2) may be simplified to:

$$\sigma_{eff} = \frac{\sigma_a(\sigma_c - i\varepsilon_0\omega)}{\sigma_a \alpha^2 + (\sigma_c - i\varepsilon_0\omega)} \quad (3)$$

As discussed previously [15], two excitations may be observed within the tilted geometry: i) a peak in the real part of the conductivity if $Im[\sigma_a \alpha^2 + (\sigma_c - i\varepsilon_0\omega_1)] = 0$ which corresponds to the mixed ab-plane/c-axis excitation and ii) the longitudinal resonance if $Im[\sigma_c - i\varepsilon_0\omega_0] = 0$ which corresponds to the c-axis plasma frequency. Both excitations have been detected for the optimally doped film #B [15]. The c-axis plasma frequency can be identified in the submillimeter frequency range also for the reduced $Nd_{1.85}Ce_{0.15}CuO_{4-\delta}$ film (see below). Due to the larger tilt angle of the sample #A the frequency of the mixed resonance is shifted to $\nu_1 \sim 200$ cm⁻¹ (compared to $\nu_1 \sim 20$ cm⁻¹ for sample #B [15]) and occurs as a broad maximum in the effective conductivity spectra at infrared frequencies [19].

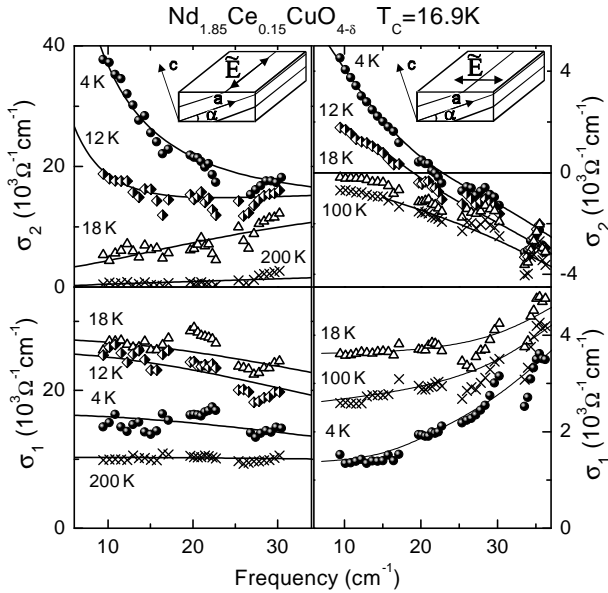


FIG. 1. Real (bottom panels) and imaginary (top panels) parts of the complex conductivity of $Nd_{1.85}Ce_{0.15}CuO_{4-\delta}$ (film #A) for different geometries of the transmission experiment as indicated in the insets. Left panels: ab-plane conductivity. Solid lines are calculated as explained in the text. Right panels: mixed conductivity. Dashed lines are guides to the eye.

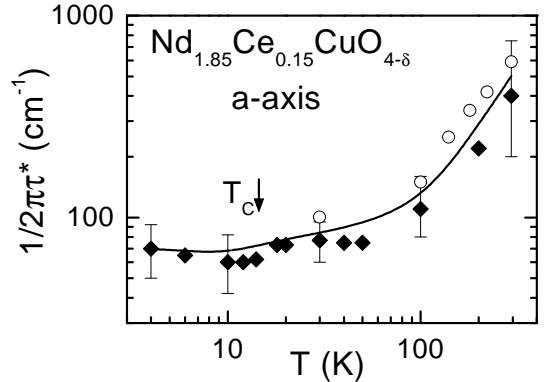


FIG. 2. In-plane quasiparticle scattering rate of $Nd_{1.85}Ce_{0.15}CuO_{4-\delta}$ film #A (full diamonds) as obtained from the Drude analysis of the complex conductivity data (left panels of Fig. 1). Open circles: infrared data from Ref. [10]. Solid line represents $1/2\pi\tau = 67$ cm⁻¹ for $T < 70$ K and $1/2\pi\tau \propto T$ for $T > 70$ K.

Fig. 1 shows the complex conductivity of the reduced $Nd_{1.85}Ce_{0.15}CuO_{4-\delta}$ film obtained as described above. The left panels represent the real (lower frame) and imaginary (upper frame) parts of the complex conductivity for currents within the CuO₂ plane. The real part of the in-plane conductivity σ_{1a} is weakly frequency-dependent in the submillimeter frequency range at all measured temperatures. This indicates that the quasiparticle scattering rate is larger than the frequency of the experiment. Consequently, the imaginary part of the conductivity σ_{2a} is nearly zero for high temperatures but starts to show distinct frequency dependence on approaching the superconducting transition temperature. From the analysis of σ_{1a} and σ_{2a} the quasiparticle scattering rate may be estimated using the Drude expression: $\sigma^* = \sigma_{dc}/(1 - i\omega\tau)$. The term $[i/\omega + \pi\delta(\omega)/2]/[\mu_0\lambda_a^2(T)]$ has to be added to the Drude expression for $T < T_C$ in order to account for the superconducting condensate [20]. Here λ_a^2 is the in-plane penetration depth, μ_0 the permeability of free space. For finite frequencies the additional term influences σ_{2a} only. The solid lines in the left panels of Fig. 1 were calculated using the Drude expression extended to temperatures below T_C as described above. The fits allow to estimate the quasiparticle scattering rate both, below and above T_C . The results are shown in Fig. 2 (full diamonds). The scattering rate is approximately constant for $T \lesssim 70$ K and shows only a small anomaly (within experimental errors) at T_C . For $T > T_C$, $1/\tau$ agrees well with the infrared data of Homes *et al.* [10] (open circles) and has an approximate linear temperature dependence for $T > 100$ K. The absence of the anomalous suppression of the quasiparticle scattering is in contrast to the results on other cuprate superconductors [21]. This possibly indicates that $1/\tau$ is determined by impurity scattering for $T \ll T_C$. For $T \ll T_C$ the $(1/\omega)$ frequency dependence dominates the imaginary part of the conductivity σ_{2a} which allows to estimate the low-frequency in-plane

penetration depth, $\lambda_a(6K) = 0.35\mu$. For the optimally doped sample #B we obtained $\lambda_a(6K) = 0.23\mu$ [15].

The right panels of Fig.1 represent the effective (mixed) conductivity which is described by Eq. (2). Using this equation, the c-axis conductivity may be calculated from the in-plane and mixed conductivity data. The imaginary part of the mixed conductivity crosses zero around $\nu \sim 20 \text{ cm}^{-1}$. As will be seen below, this frequency corresponds to the c-axis plasma resonance.

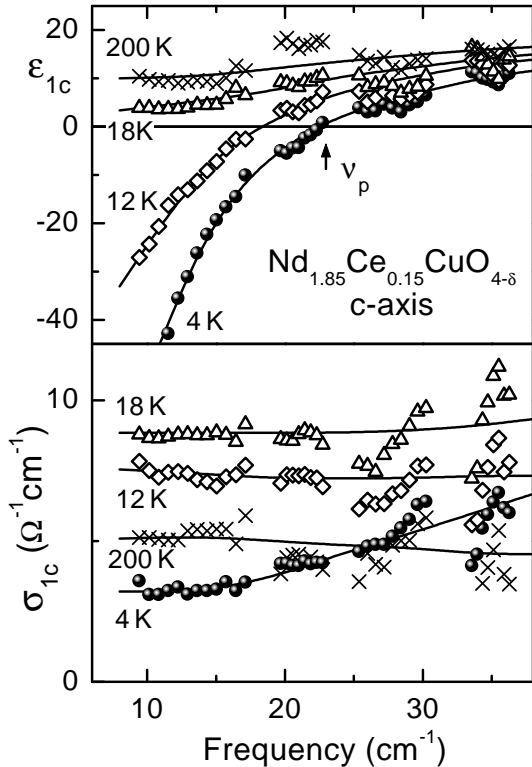


FIG. 3. Conductivity σ_{1c} (bottom panel) and dielectric constant $\varepsilon_{1c} = -\sigma_{2c}/(\varepsilon_0\omega)$ (top panel) of $\text{Nd}_{1.85}\text{Ce}_{0.15}\text{CuO}_{4-\delta}$ (sample #A) along the c-axis. Lines are guides to the eye. Arrow indicates the position of the c-axis plasma frequency.

Fig.3 shows the conductivity σ_{1c} and the dielectric constant $\varepsilon_{1c} = -\sigma_{2c}/(\varepsilon_0\omega)$ of $\text{Nd}_{1.85}\text{Ce}_{0.15}\text{CuO}_{4-\delta}$ (#A) along the c-axis. The real part of the c-axis conductivity (lower frame) is approximately frequency independent within experimental accuracy and for temperatures well above T_C . This behavior agrees well with the low-frequency infrared conductivity of $\text{La}_{2-x}\text{Sr}_x\text{CuO}_4$ [22,23], $\text{YBa}_2\text{Cu}_3\text{O}_{6.7}$ [24], and $\text{Tl}_2\text{BaCuO}_{6+x}$ [25]. Only at the lowest temperatures σ_{1c} does increase with frequency which most probably reflects the vicinity of the c-axis phonon at $\nu \approx 134 \text{ cm}^{-1}$ [14,19]. The c-axis dielectric constant is dominated by the high-frequency (phonon) contribution and shows a weak frequency dependence at high temperatures. As the sample becomes superconducting, ε_{1c} reveals a $(1/\omega^2)$ behavior, which gives an estimate of the penetration depth, $\lambda_c(6K) =$

19.2μ . Consequently, a zero crossing of ε_{1c} is observed around 20 cm^{-1} which corresponds to the (screened) plasma frequency $2\pi\nu_p = c/(\lambda_c\varepsilon_\infty^{1/2})$ where $\varepsilon_\infty \approx 14$ is the high-frequency dielectric constant and c is the speed of light. For the sample #B we found $\nu_p = 12\text{cm}^{-1}$ and $\varepsilon_\infty \approx 23$ [15].

Assuming Josephson coupling between the CuO_2 planes, Basov *et al.* [26] suggested a correlation between $\lambda_c(0)$ and the normal-state conductivity $\sigma_c(T_C) : \hbar/(\mu_0\lambda_c^2) = \pi\Delta\sigma_c(T_C)$. On the basis of this correlation the results on both NCCO samples give an energy gap $2\Delta \simeq 30 \text{ cm}^{-1}$. This value may be compared to $2\Delta \simeq 60 \text{ cm}^{-1}$ as determined by Raman scattering [27].

The temperature dependence of the anisotropic conductivity, as measured at $\nu = 10 \text{ cm}^{-1}$, is represented in Fig. 4. The lower panel of Fig. 4 shows the real and imaginary parts of the in-plane conductivity. For decreasing temperature, σ_{1a} increases below room temperature, saturates between $T \simeq 100 \text{ K}$ and T_C and finally decreases after a slight maximum near T_C . A peak near T_C observed in σ_{1a} at microwave frequencies was recently reported for NCCO by Kokales *et al.* [5] and interpreted as possible evidence for suppression of the quasiparticle scattering. According to Fig. 2, our data suggest a rather temperature independent scattering of quasiparticles below $T = 100 \text{ K}$. At high temperatures the imaginary part of the in-plane conductivity (lower panel of Fig. 4, open triangles) has values just above the sensitivity limit of the spectrometer. In the superconducting state σ_{2a} abruptly increases reflecting the formation of the superconducting condensate.

The lower panel of Fig. 4 shows the comparison of the experimental conductivity with theoretical models. As representative examples we have taken the s-wave BCS expression, as well as Born ($\tilde{\sigma} = 0$) and unitary ($\tilde{\sigma} = 1$) limits of a d-wave superconductor [28]. Here $\tilde{\sigma}$ is the cross section of the impurity scattering. All three models calculate a gap value self-consistently within the weak coupling limit and assume a *temperature independent* quasiparticle scattering rate of $1/2\pi\tau = 65 \text{ cm}^{-1}$. It has to be pointed out, that real and imaginary parts of the conductivity have to be fitted simultaneously below and above T_C . This condition leaves *no free parameters* within the models. As documented by the fit results in Fig. 4, the s-wave curve (solid line) shows the poorest agreement with the experiment. In contrast, both limits of the d-wave model describe σ_{1a} reasonably well. However, the unitary limit (dotted) substantially underestimates the imaginary part σ_{2a} . This is probably because in this limit less spectral weight is shifted to the δ -function at zero frequencies [28]. The best description of σ_{2a} may be obtained using an intermediate scattering cross section $\tilde{\sigma} \simeq 0.2$. Similar results have been obtained for the optimally doped sample #B for which $\tilde{\sigma} = 0$ gave the best description of the data.

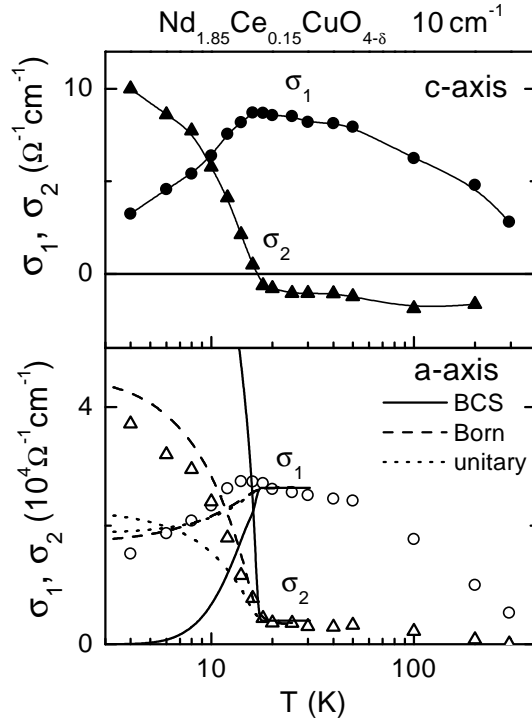


FIG. 4. Temperature dependence of the complex conductivity of $\text{Nd}_{1.85}\text{Ce}_{0.15}\text{CuO}_{4-\delta}$ film #A at $\nu = 10 \text{ cm}^{-1}$. Upper panel: c-axis. Lines are guides to the eye. Lower panel: ab-plane. Lines are calculated according to the s-wave BCS model (solid), Born (dashed) and unitary (dotted) limits of the d-wave model [28].

The upper panel of Fig. 4 shows the temperature dependence of the c-axis conductivity of $\text{Nd}_{1.85}\text{Ce}_{0.15}\text{CuO}_{4-\delta}$. Except for the absolute values, these data closely follow the temperature dependence of the in-plane conductivity. The most prominent difference is caused by the strong phonon contribution on the c-axis conductivity, evidenced by a downward shift of σ_{2c} . Based on the strong in-plane momentum dependence of the scattering rate and of the hopping integral, the anisotropic conductivity for high- T_C cuprates was recently calculated by van der Marel [29], and Xiang and Hardy [30]. Parametrizing the in-plane momentum by an angle θ and using $t_c = -t_{\perp} \cos^2(\theta)$ for the c-axis hopping integral, the c-axis conductivity was found to behave as $\sigma_{1c} \propto T^3$ for not too low temperatures [30]. The analysis of Fig. 4 shows, that σ_{1c} as well as σ_{1a} for NCCO depend rather linear on temperature below T_C . The explanation for this behavior probably is an impurity-induced angular-independent contribution to t_c . Following the calculations described in Refs. [29,30] this correction does indeed give a linear temperature dependence of the c-axis conductivity [31].

In conclusion, the anisotropic conductivity of $\text{Nd}_{1.85}\text{Ce}_{0.15}\text{CuO}_{4-\delta}$ films has been obtained using the tilted-sample geometry in the frequency range $8 \text{ cm}^{-1} < \nu < 40 \text{ cm}^{-1}$ and for temperatures 4 K

$< T < 300 \text{ K}$. The in-plane scattering rate is shown to be unchanged as the sample becomes superconducting. The temperature dependence of the in-plane conductivity may be reasonably described within the Born limit of a dirty d-wave superconductor. The c-axis dielectric constant ϵ_{1c} is dominated by a phonon contribution at high temperatures. A zero crossing of ϵ_{1c} is directly observed below T_C which corresponds to the screened c-axis plasma frequency. In contrast to other cuprate superconductors, the temperature dependence of the c-axis conductivity closely follows the in-plane behavior.

This work was supported by BMBF (13N6917/0 - EKM) and in part by the Deutsche Forschungsgemeinschaft through SFB 484.

- [1] Y. Tokura *et al.*, *Nature* **337**, 345 (1989).
- [2] Y. Hidaka and M. Suzuki, *Nature* **338**, 635 (1989).
- [3] P. Fournier *et al.*, in *Gap Symmetry and Fluctuations in High-T_C Superconductors*, edited by J. Bok *et al.*, (Plenum Press, NY, 1998), p.145.
- [4] C. C. Tsuei and J. R. Kirtley, cond-mat/0002341.
- [5] J. D. Kokales *et al.*, preprint cond-mat/0002300.
- [6] R. Prozorov *et al.*, preprint cond-mat/0002301.
- [7] A. Andreone *et al.*, *Phys. Rev. B* **49**, 6392 (1994).
- [8] S. M. Anlage *et al.*, *Phys. Rev. B* **50**, 523 (1994).
- [9] D.-H. Wu *et al.*, *Phys. Rev. Lett.* **70**, 85 (1993).
- [10] C. C. Homes *et al.*, *Phys. Rev. B* **56**, 5525 (1997).
- [11] S. Lupi *et al.*, *Phys. Rev. Lett.* **83**, 4852 (1999).
- [12] E.-J. Choi *et al.*, *Phys. Rev. B* **53**, 8859 (1996).
- [13] H. Shibata and T. Yamada, *Phys. Rev. B* **54**, 7500 (1996); *ibid.* **56**, 14275 (1997).
- [14] E. T. Heyen *et al.*, *Sol. State Comm.* **74**, 1299 (1990).
- [15] A. Pimenov *et al.*, preprint cond-mat/0003404.
- [16] Beom-hoan O and J. T. Markert, *Phys. Rev. B* **47**, 8373 (1993).
- [17] V. S. Nozdrin *et al.*, *Tech. Phys. Lett.* **22**, 996 (1996).
- [18] A. A. Volkov *et al.*, *Infrared Phys.* **25**, 369 (1985).
- [19] A. V. Pronin *et al.*, unpublished.
- [20] A. Pimenov *et al.*, *Phys. Rev. B* **61**, 7039 (2000).
- [21] D. A. Bonn and W. N. Hardy in *Physical Properties of High Temperature Superconductors V*, edited by D. M. Ginsberg (World Scientific, Singapore, 1996), p. 7.
- [22] S. Uchida *et al.*, *Phys. Rev. B* **53**, 14558 (1996).
- [23] J. H. Kim *et al.*, *Physica C* **247**, 297 (1995).
- [24] C. C. Homes *et al.*, *Phys. Rev. Lett.* **71**, 1645 (1993).
- [25] D. N. Basov *et al.*, *Science* **283**, 49 (1999).
- [26] D. N. Basov *et al.*, *Phys. Rev. B* **50**, 3511 (1994).
- [27] B. Stadlober *et al.*, *Phys. Rev. Lett.* **74**, 4911 (1995).
- [28] M. J. Graf *et al.*, *Phys. Rev. B* **52**, 10588 (1995).
- [29] D. van der Marel, *Phys. Rev. B* **60**, 765 (1999).
- [30] T. Xiang and W. N. Hardy, preprint cond-mat/0001443.
- [31] U. Michelucci *et al.*, unpublished.